 doi:10.20944/preprints202006.0222.v1

Article

Astaxanthin Prevents Atrophy in Slow Fiber Muscles by Inhibiting Mitochondrial Reactive Oxygen Species Via a Mitochondria-Mediated Apoptosis Pathway

Luchuanyang Sun[1], Nobuyuki Miyaji[2], Min Yang[1], Edward M. Mills[3], Shigeto Taniyama[1], Takayuki Uchida[4], Takeshi Nikawa[4], Jifeng Li[5], Jie Shi[5], Katsuyasu Tachibana[1] and Katsuya Hirasaka[1, 6, *]

[1] Graduate School of Fisheries and Environmental Sciences, Nagasaki University, Nagasaki, Japan 8528521; slcywelcome@126.com (L.S.); 18342221707@163.com (M.Y.); tshigeto@nagasaki-u.ac.jp (S.T.); orenge@nagasaki-u.ac.jp (K.T.)
[2] Toyo Koso Kagaku Co. Ltd., Chiba, Japan 2790041; miyaji@toyokk.co.jp (N.M.)
[3] Division of Pharmacology/Toxicology, University of Texas at Austin, Austin, TX USA 78712; tedmills@austin.utexas.edu (E. M. M)
[4] Department of Nutritional Physiology, Institute of Medical Nutrition, Tokushima University Medical School, Tokushima, Japan 7708503; t.uchida@tokushima-u.ac.jp (T.U.); nikawa@tokushima-u.ac.jp (T.N.)
[5] Weihai lida biological technology Co., Ltd., China 264200; lijifeng6812@gmail.com (J.L.); shijie.lida@gmail.com (J.S.)
[6] Organization for Marine Science and Technology, Nagasaki University, Nagasaki, Japan 8528521; hirasaka@nagasaki-u.ac.jp (K.H.)
* Correspondence: hirasaka@nagasaki-u.ac.jp (K.H.); Tel.: +81-(95) 819-2839

Abstract: Astaxanthin (AX) is a carotenoid that exerts potent antioxidant activity and acts in the lipid bilayer. This study aimed to investigate the effects of AX on muscle atrophy-mediated disturbance of mitochondria that have a lipid bilayer. Tail suspension was used to establish muscle-atrophied mouse models. AX diet fed to tail-suspension mice prevented loss of muscle weight and decreased myofiber size in the soleus muscle. Additionally, AX improved down-regulation of mitochondrial respiratory chain complexes II and III in the soleus muscle after tail suspension. To confirm the AX phenotype in the soleus muscle, we examined its effects on mitochondria using Sol8 myotubes derived from the soleus muscle. We found that AX was preferentially detected in the mitochondrial fraction; it significantly suppressed mitochondrial complex III-driven production of reactive oxygen species in Sol8 myotubes. Moreover, AX inhibited the activation of caspase 3 via inhibiting the release of cytochrome c into the cytosol in antimycin A-treated Sol8 myotubes. These results suggested that AX inhibited mitochondrial oxidative stress through a mitochondria-mediated apoptosis pathway and thus prevented muscle atrophy.

Keywords: astaxanthin; muscle atrophy; mitochondria; oxidative stress

1. Introduction

Skeletal muscle atrophy has been observed in muscle disuse during unloading, immobilization, denervation, fasting, aging, and several disease conditions. Unloading-related muscle loss caused by prolonged bed rest or spaceflight specifically occurs in antigravity muscles including slow fiber muscles [1, 2]. It has been known that the number of mitochondria in slow fiber muscle is higher than that in fast fiber muscle [3]. Mitochondria are the main energy source of skeletal muscles that produce adenosine triphosphate (ATP) through oxidative phosphorylation (OXPHOS). In this process, 0.2–2.0% of diatomic oxygen passes through the electron transport chain complexes I and III and incompletely reduces leaked electrons to superoxide anions [4]. Excessive reactive oxygen species (ROS) including superoxide anions produced by mitochondria play a vital role in disused skeletal

Preprints (www.preprints.org) | NOT PEER-REVIEWED | Posted: 17 June 2020 doi:10.20944/preprints202006.0222.v1

muscle atrophy [5, 6]. Therefore, the development of antioxidants to prevent the increase in mitochondrial ROS in muscle due to inactivity has been extensively researched.

Astaxanthin (AX; 3,3′-dihydroxy-β, β′-carotene-4,4′-dione), a ketone carotenoid with 13 conjugated double bonds, naturally accumulates in microalgae, yeast, crustaceans, fish epidermis, and other biologicals. Natural AX is mainly obtained from *Haematococcus pluvialis* and its biological effects as an antioxidant have been widely studied [7]. The unique molecular structure of AX allows for its insertion through the lipid bimolecular layer of cell membranes, leading to stronger protection and free radical scavenging effects at the cell membrane than other antioxidants such as β-carotene, α-tocopherol, and vitamin C [8, 9]. AX reportedly maintains mitochondrial integrity by reducing oxidative stress, prevents the loss of mitochondrial membrane potential, and increases mitochondrial oxygen consumption, which inhibits mitochondrial dysfunction [10-12]. Additionally, AX suppresses bleomycin-induced ROS generation and apoptosis mediated by the disturbed mitochondrial signaling pathway in type II alveolar epithelial cells [13]. These reports raise the possibility that AX acts in both the mitochondrial and cell membranes.

Although antioxidants have been shown to prevent muscle atrophy [14, 15], their mechanisms of action vary owing to their different characteristics. Some studies have shown that AX might have an effect on muscle atrophy [16, 17]; however, its mechanism of action in mitochondria remains unclear. This study investigated the effect of AX on muscle atrophy induced by mitochondrial oxidative stress and dysfunction. Sol8 cells (slow-type muscle cells extracted from soleus muscle) were used to explore the underlying mechanisms.

2. Materials and Methods

2.1 Animal model

Male C57BL/6J mice (Japan CLEA, Tokyo, Japan) (5 weeks old) were housed in a room maintained at 24 ± 1°C and a 12-h light/dark cycle with food (Oriental Yeast Company, Tokyo, Japan) and water available ad libitum. After 1 week of acclimation, mice were randomized into 4 groups: control mice fed the normal diet (C-ND, n = 6); tail-suspension mice fed the normal diet (S-ND, n = 6); control mice fed the AX diet (C-AX, n = 6); and tail-suspension mice fed the AX diet (S-AX, n = 6). An AX-supplemented (0.2%, w/w) or a normal diet was fed to mice for four weeks. Then, they were subjected to tail suspension to establish the muscle atrophy model. Briefly, the mouse tail was fixed with medical tape; the other end of the tape attached to the top of the cage to keep its body at a 30° angle with the surface. The forelimbs were free to move on the ground to enable free access to water. During the development of tail suspension-induced muscle atrophy, the mice continued to receive normal or AX-supplemented diets until termination of the experiment two weeks later. The soybean oil content of the AX-supplemented diet was reduced to adjust for the composition of other nutrients. The AX-supplemented diet comprised the normal diet (based on AIN-93G) mixed with Bio Astin SCE (containing 10% AX; Toyo Koso Kagaku Co. Ltd., Chiba, Japan). The nutritional composition of each diet is shown in Table S1. Right hindlimb skeletal muscles including the tibialis anterior (TA), extensor digitorum longus (EDL), gastrocnemius (GA), and soleus (SO) muscles were isolated at the time of sacrifice. After measuring the wet weight, the skeletal muscles were immediately frozen in chilled isopentane with liquid nitrogen and stored at -80°C until analysis. All animal experiments were approved by the Committee on Animal Experiments of Nagasaki University (Permission No. 1803291443) and performed according to the guidelines for the care and use of laboratory animals set by the University.

2.2 Multicolor immunofluorescence staining and measurement of cross-sectional area (CSA)

Sections of the SO muscle (5 μm thickness) were fixed in ice-cold acetone and stained using multicolor immunofluorescence antibodies as described previously [18]. Primary antibody reactions were performed using anti-myosin heavy chain (MHC) type I (BA-F8), anti-MHC IIa (SC-71), and anti-MHC IIb (BF-F3) (DSHB, Iowa City, IA, USA); the secondary antibodies used were anti-mouse Alexa Fluor 350 IgG_{2b}, anti-mouse Alexa Fluor 488 IgG_1, and anti-mouse Alexa Fluor 555 IgM, respectively (Thermo Fisher Scientific, Waltham, MA, USA). Images were acquired using a BIOREVO

Preprints (www.preprints.org) | NOT PEER-REVIEWED | Posted: 17 June 2020 doi:10.20944/preprints202006.0222.v1

BZ-X710 microscope (Keyence, Osaka, Japan). For fiber type analysis, all fibers within the entire cross-section were characterized. At least 600 myofiber cross-sectional areas (CSAs) were measured per group. The data are expressed as fiber size distribution.

2.3 Cell culture

Sol8 myoblastic cells were obtained from the American Type Culture Collection (ATCC, Manassas, VA). They were cultured in Dulbecco's modified Eagle medium (DMEM) supplemented with 10% fetal bovine serum (FBS), 100 units/mL penicillin, and 100 μg/mL streptomycin and maintained at 37°C in a 5% CO_2 environment. At a confluence of 100%, Sol8 myoblasts were fused by shifting the medium to DMEM supplemented with 2% horse serum (HS). Cells were maintained in 2% HS/DMEM (differentiation medium) for 4 days for the formation of myotubes, prior to their use in experiments.

2.4. Detection of AX in mitochondrial and cytosolic fractions

The AX contents in mitochondrial and cytosolic fractions from Sol8 myotubes were prepared, as described previously [19]. Briefly, Sol8 myotubes were treated with AX (100 pmol) or DMSO, as control, in 100 mm dishes and incubated at 37°C with 5% CO_2 for 24 h. The cells were harvested and immediately minced in ice-cold CP-1 buffer (100 mM KCl, 50 mM Tris-HCl, 2 mM EGTA; pH 7.4), homogenized, then centrifuged at 500 × *g* for 10 min. The supernatant was collected and further centrifuged for 10 min at 10,500 × *g* to obtain the mitochondrial pellet and cytosolic fraction. After lyophilization, crude mitochondrial extracts and cytosol were solubilized in acetone and centrifuged at 12,000 × *g* for 15 min. The supernatants were filtered using a 0.45 μm polytetrafluorethylene membrane and analyzed using HPLC and a spectrophotometer detector (JASCO, Tokyo, Japan) set at 460 nm. A Shim-pack CLC-ODS column (150 mm length and 6.0 mm internal diameter) was used.

2.5 Measurement of mitochondrial ROS and mitochondrial membrane potential (MMP)

Mitochondrial ROS levels were detected using a fluorescent probe, dihydroethidium (DHE), as described previously [20]. Differentiated Sol8 myotubes were plated in 96-well black plates and treated with DMSO or AX for 24 h. The cells were then incubated with HBSS containing 10 mM succinate, 10 μM antimycin A, and 5 μM DHE. Fluorescence was recorded using a microplate reader (BioTek Cytation 3, Winooski, VT, USA) at excitation and emission wavelengths of 490 and 595 nm, respectively.

MMP was detected using the fluorescent probe, JC-1 dye (Thermo Fisher Scientific). Differentiated Sol8 myotubes were plated in 96-well black plates and pretreated with DMSO or AX for 1 h, followed by the addition of 25 μM antimycin A for 48 h. After washing by PBS, the cells were incubated with 1.5 μM JC-1 dye at 37°C for 30 min. MMP was quantified using a microplate reader (BioTek Cytation 3) at 550 nm excitation/ 600 nm emission and 485 nm excitation/ 535 nm emission wavelengths. The quantitative MMP value was expressed as the relative ratio of aggregate-to-monomer values of fluorescence intensity. Carbonyl cyanide m-chlorophenyl hydrazone (CCCP) was used as a negative control to normalize changes in the membrane.

2.6 Immunoblotting

Mouse SO muscles and Sol8 were prepared in 50 mM Tris-HCl, pH 8.0, containing 1% NP40, 0.5% sodium deoxycholate, 0.1% SDS, 150 mM NaCl, 2 mM EDTA, and protease inhibitors (Roche Diagnostics, Tokyo, Japan) and homogenized using a sonicator. The cytosolic fraction for the analysis of cytochrome c release was prepared as described in section 2.4. The Pierce BCA assay (Pierce, Rochford, IL, USA) was used to quantify proteins. Protein samples were combined with 4X sample buffer (250 mM Tris-HCl, 8% SDS, 40% glycerol, 8% beta-mercaptoethanol, and 0.02% bromophenol blue) and subjected to SDS-PAGE. The proteins were transferred onto a polyvinylidene difluoride (PVDF) membrane and probed with primary antibodies according to the manufacturer's instructions. Anti-β-actin (Gene Tex, AC-15, Irvine, CA), anti-cleaved caspase 3 (Cell Signaling Technology, #9661, Danvers, MA), anti-caspase 3 (Cell Signaling Technology, #9662, Danvers, MA), anti-cytochrome c (Santa Cruz Biotechnology, sc-13156, Santa Cruz, CA), anti-GAPDH (Santa Cruz Biotechnology, sc-

Preprints (www.preprints.org) | NOT PEER-REVIEWED | Posted: 17 June 2020 doi:10.20944/preprints202006.0222.v1

25778), and anti-total OXPHOS (Abcam, ab110413, Cambridge, UK) were used. Donkey anti-rabbit IgG at 1:5000 (GE Healthcare, Little Chalfont, UK) and sheep anti-mouse IgG at 1:5000 (GE Healthcare) were used as the secondary antibodies. Membranes were developed using ImmunoStar®Zeta western blotting detection reagents (Fujifilm Wako Pure Chemical Corporation, Osaka, Japan).

2.7 Statistical analyses

All data were analyzed using one-way analysis of variance using Excel-Toukei version 6.0 software (Statistics Survey System-development, Tokyo, Japan), followed by Tukey's test for individual group differences. All data are expressed as the mean ± S.E., n = 3–8. *P*-values < 0.05 were considered to indicate significant differences.

3. Results

3.1 Effect of dietary AX on muscle mass and fiber size distribution in tail-suspension mice

To examine the effect of AX on weight gain in mice, we compared the body and wet weights of several muscles of the normal control and tail-suspension mice fed a normal or AX-supplemented diet. There was no significant difference between the normal and AX-supplemented diet groups in food intake (Figure 1a). Although the body weights of mice in the S-ND and S-AX groups significantly decreased after tail-suspension, these differences were not significant (Figure 1b).

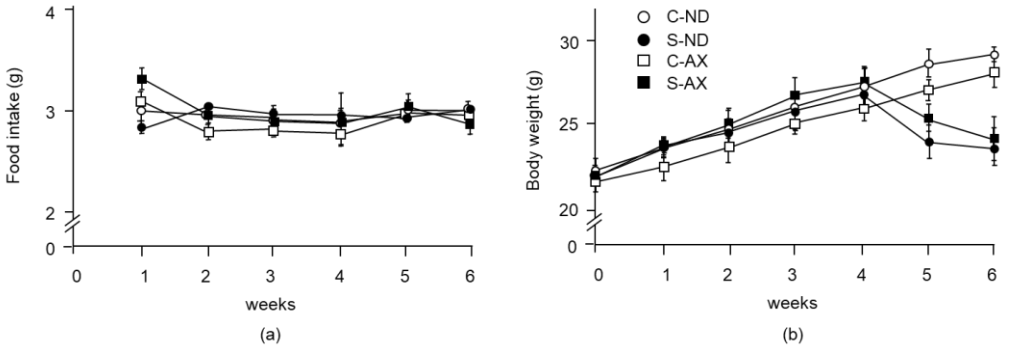

Figure 1. Changes in food intake and body weight with the AX diet: **(a)** food intake; **(b)** body weight. Mice were fed an AX or normal diet for 6 weeks. They were subjected to tail suspension at 4 weeks, which continued for 2 weeks (C-ND, n = 6; S-ND, n = 6; C-AX, n = 6; S-AX, n = 6). C-ND, control mice fed a normal diet; S-ND, tail-suspension mice fed a normal diet; C-AX, control mice fed the AX diet; and S-AX, tail-suspension mice fed the AX diet.

Tail suspension significantly decreased the weights of TA, GA, and SO muscles, but not that of EDL (Figure 2). In comparison to the S-ND group, the S-AX group showed inhibition of muscle-weight reduction only in the SO. In contrast, AX supplementation failed to prevent tail suspension-induced muscle atrophy in the EDL, TA, and GA muscles.

Preprints (www.preprints.org) | NOT PEER-REVIEWED | Posted: 17 June 2020 doi:10.20944/preprints202006.0222.v1

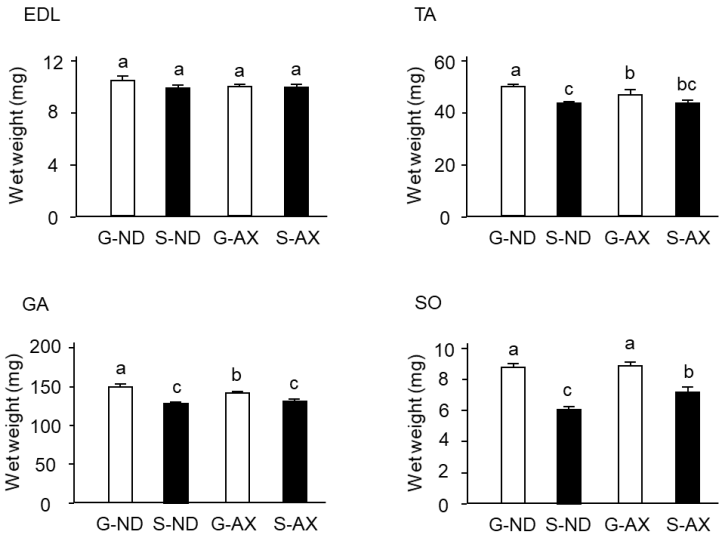

Figure 2. The effect of dietary AX on the tail-suspension induced decreased in the wet weight of skeletal muscle. An AX-supplemented or normal diet was given to the mice for 4 weeks and their skeletal muscles were isolated 2 weeks after tail suspension. The wet weights of the tibialis anterior, extensor digitorum longus, gastrocnemius, and soleus muscles were measured. Data are presented as mean ± S.E. (n = 6). Different letters indicate significant differences ($P < 0.05$) based on ANOVA and Tukey's test. C-ND, control mice fed the normal diet; S-ND, tail-suspension mice fed the normal diet; C-AX, control mice fed the AX diet; and S-AX, tail-suspension mice fed the AX diet.

Next, we analyzed the cross-sectional area (CSA) of the SO muscle fiber. Multicolor immunofluorescent staining showed that it comprised MHC types I (blue) and IIa (green) myofibers. Type IIb (red) myofibers were hardly detected in the SO muscle fibers. Myofibers in the S-ND group showed decreased CSA staining and comprised types I and IIa (Figure 3a), compared to the C-ND group. In contrast, the CSAs of muscle fibers stained with types I and IIa in the S-AX mice were similar to those observed in the C-AX mice (Figure. 3a). We confirmed the distribution of types I and IIa fibers in the SO muscle. Consistent with the results that indicated a decrease in muscle weights in the S-ND group, the size distribution of types I and IIa muscle fibers in the S-ND group showed a leftward shift compared to the C-ND group. Meanwhile, the size distribution of both in muscle fibers in the S-AX group was almost the same as that in the C-ND and C-AX groups (Figure. 3b). In particular, tail suspension in the S-AX group showed no leftward shift in the size distribution of muscle fibers of MHC types I and IIa.

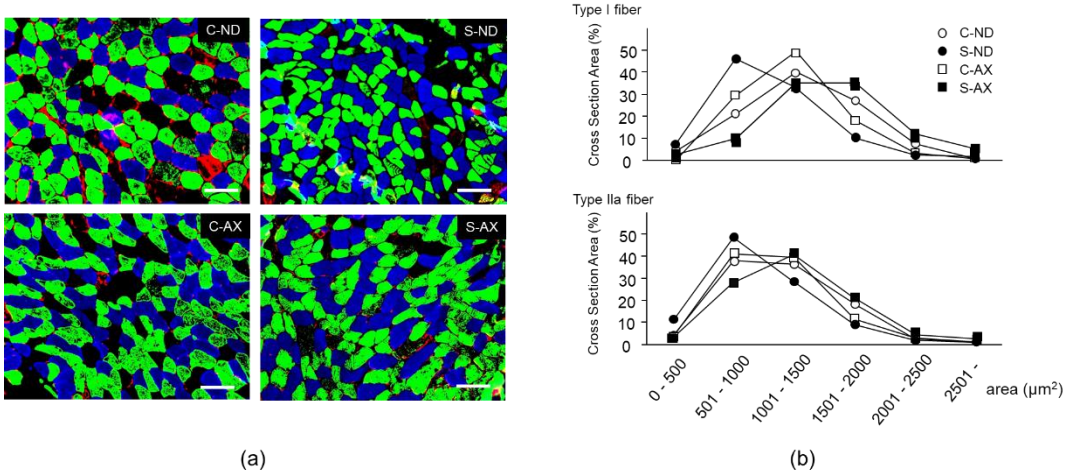

Figure 3. Effect of dietary AX on the tail-suspension induced decrease in muscle cross-sectional area (CSA). **(a)** Sections (5-μm thickness) of SO muscle from C-ND, C-AX, S-ND, and S-AX groups, with multicolor immunofluorescence staining. Scale bar = 100 μm; **(b)** The CSA distributions indicate the

Preprints (www.preprints.org) | NOT PEER-REVIEWED | Posted: 17 June 2020 doi:10.20944/preprints202006.0222.v1

ratio of muscle fibers numbers, with the indicated area to the total number of muscle fibers in the section. C-ND, control mice fed the normal diet; S-ND, tail-suspension mice fed the normal diet; C-AX, control mice fed the AX-supplemented diet; and S-AX, tail-suspension mice fed the AX-supplemented diet.

3.2 Effect of dietary AX on oxidative phosphorylation respiration in the muscle of tail-suspension mice

Denervation-induced muscle atrophy reportedly impairs oxidative phosphorylation complex proteins in mitochondria [21]. We investigated the effect of AX on the levels of oxidative phosphorylation-related protein complexes in the muscle. The amounts of complexes II and III in the SO muscle of the S-ND group were significantly lower than that of the C-ND group. In contrast, there were no significant changes between the protein complexes in the C-AX and S-AX groups (Figure. 4).

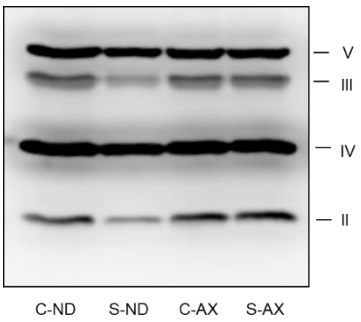

Figure 4. Effect of AX on the expression of oxidative phosphorylation-related protein complexes in SO muscle of tail-suspension mice. Proteins (20 μg/lane) were extracted from the SO muscle and subjected to SDS-PAGE and transferred onto a PVDF membrane. Immunoblotting for total OXPHOS was performed. C-ND, control mice fed the normal diet; S-ND, tail-suspension mice fed the normal diet; C-AX, control mice fed the AX-supplemented diet; and S-AX, tail-suspension mice fed the AX-supplemented diet.

3.3 Effect of AX on mitochondrial function in Sol8 myotubes

Manabe et al. reported that AX is more likely to accumulate in the mitochondria of mesangial cells [22]. This finding and the results of our *in vivo* experiments implied that AX may affect mitochondrial oxidative phosphorylation. First, we determined whether AX was detected in the mitochondrial fraction using Sol8 myotubes. We found that AX was preferentially detected in the mitochondrial fraction, which was approximately 1% that of the AX treatment concentration in Sol8 myotubes; DMSO (0 pmol AX) was detected neither in the mitochondria nor cytosol (Table 1). This result was consistent with a previous report that AX is more likely to accumulate in the mitochondria in mesangial cells [22].

Table 1. AX content in mitochondria and cytosol of AX-treated Sol8 myotubes

AX treatment	AX content (pmol)	
	Cytosol	Mitochondria
0 pmol	N.D.	N.D.
100 pmol	0.09 ± 0.01	1.07 ± 0.02

Data are presented as mean ± S.E. (n = 3). N.D.: not detected

Next, we analyzed the effect of AX on mitochondrial ROS generation and MMP levels in Sol8 myotubes treated with antimycin A (AnA), a complex III inhibitor. Mitochondrial ROS production in AnA-treated Sol8 myotubes was significantly increased compared to that in non-treated cells. The increased production of complex III-driven ROS was significantly suppressed by AX treatment in a dose-dependent manner (Figure. 5a). Addition of AX in AnA non-treated Sol8 myotubes did not influence MMP (Figure. 5b). AnA treatment significantly decreased the MMP in Sol8 myotubes relative to non-treated cells, resulting in the same MMP level as that of the negative control, with the

Preprints (www.preprints.org) | NOT PEER-REVIEWED | Posted: 17 June 2020 doi:10.20944/preprints202006.0222.v1

uncoupler CCCP. Nevertheless, improvements in MMP levels were noticed in the AX-treated cells, although there were no significant differences between the different AX concentrations. These results suggested that AX pretreatment may inhibit mitochondrial ROS production and maintain the MMP in Sol8 myotubes, thereby inhibiting induced cell death. These results indicated that the role of AX in mitochondrial protection.

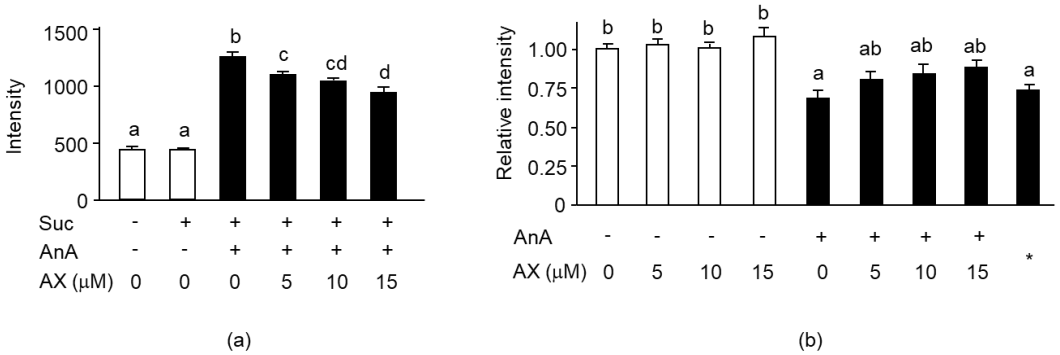

Figure 5. Effect of AX on mitochondrial ROS production and MMP in AnA-treated sol8 myotubes: **(a)** The rate of superoxide formation in AX-treated Sol8 myotubes was assessed using DHE fluorescence. Succinate and AnA were used as respiratory complex II substrate and complex III inhibitor, respectively; **(b)** The quantitative MMP values were calculated based on the ratio of fluorescence intensity values (JC-1 dye). Data are represented as mean ± S.E. (n=8). Different letters indicate significant differences ($P < 0.05$) based on ANOVA and Tukey's test. "-" represents DMSO; *, CCCP; Suc, succinate; AnA, antimycin A.

3.4 The effect of AX on the expression of apoptosis-related proteins in AnA-treated Sol8 myotubes

To explore the mitochondria-mediated apoptotic mechanism of AX in AnA-treated Sol8 myotubes, the release of cytochrome c into the cytosol (Figure. 6a) and activation of caspase 3 (Figure. 6b) were examined. The amount of cytochrome c in AnA-treated Sol8 myotubes, without AX, in the cytosolic fraction was significantly increased compared to the DMSO-treated control group (Figure. 8). In contrast, AX inhibited the release of cytochrome c into the cytosol of AnA-treated Sol8 myotubes. Furthermore, AnA treatment tended to increase the amount of cleaved caspase 3 in Sol8 myotubes, whereas AX effectively decreased the amount of cleaved caspase 3 in AnA-treated Sol8 myotubes (Figure. 6b).

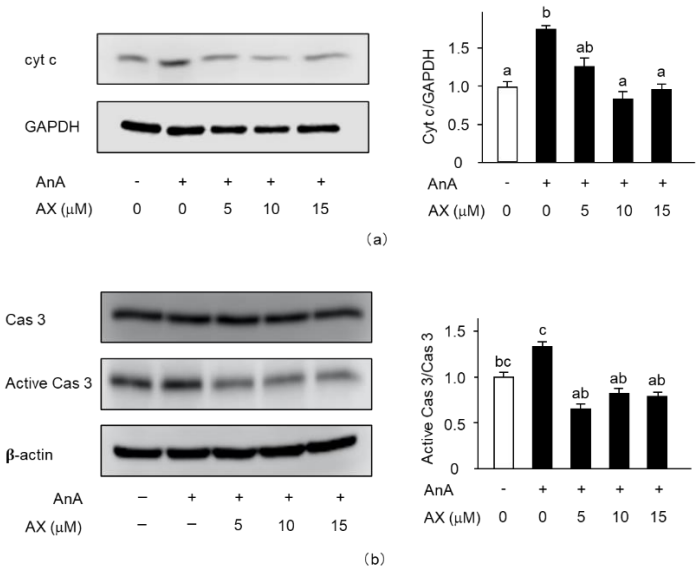

Figure 6. Effect of AX on the activation of apoptosis-related proteins in AnA-treated Sol8 myotubes: **(a)** Sol8 myotubes were treated with different AX concentrations for 1 h, then AnA (25 μM) was added

for 48 h. The cytosolic fraction was subjected to SDS-PAGE and transferred onto a PVDF membrane. Immunoblotting for cyt c and GAPDH was performed on different membranes without antibody stripping, as described in section *2.6*. The ratio of cyt c proteins to GAPDH was calculated using densitometric analysis; **(b)** Sol8 myotubes were treated with different AX concentrations for 1 h and with AnA (25 μM) for 48 h before total proteins were extracted. Proteins (20 μg/lane) were extracted from Sol8 myotubes and subjected to SDS-PAGE, then transferred onto a PVDF membrane. Immunoblotting for cyt c, cas 3, and active cas 3 was performed on different membranes without antibody stripping, as described in section *2.6*. Data are presented as mean ± S.E. (n = 3). Different letters indicate significant differences ($P < 0.05$) based on ANOVA and Tukey's test. AnA, antimycin A; cyt c, cytochrome c; and cas 3, caspase 3.

4. Discussion

The novel findings of this research revealed that dietary AX supplementation attenuated the decrease in muscle mass and myofibers in the SO muscle, preventing mitochondrial dysfunction caused by oxidative stress. AX particularly inhibited the reduction of mitochondrial complexes II and III protein content in the SO muscle of tail-suspension mice. In addition, AX treatment mitigated the generation of mitochondrial complex III-derived ROS, cytochrome c release into the cytosol, and caspase 3 activation in Sol8 myotubes.

Although the body weight of mice decreased after tail suspension, EDL muscle weight did not influence this induction. This meant that muscle atrophy induced by tail suspension was not due to decreased body weight stemming from starvation. Indeed, numerous studies demonstrate that the weight loss in EDL is hardly detectable in suspended animals [23, 24]. Consistent with these findings, tail suspension induced a loss of skeletal muscle, including GA, TA, and SO, but not the EDL muscle (Figure. 2). Thus, muscle atrophy caused by tail suspension preferentially affected slow-type rather than fast-type fibers.

Numerous studies have demonstrated that mitochondria play an important role in muscle atrophy [6, 25-28]. In oxidative phosphorylation, mitochondrial respiratory chain complexes I and III are believed to be the major sites of ROS leakage, although other components of oxidative phosphorylation also contribute to the production of ROS in the mitochondria [29, 30]. We found that there was a significant reduction in mitochondrial respiratory chain complexes II and III in the SO muscle of S-ND group, compared to the C-ND group (Figure.4). Kanazashi et al. reported that the SO muscle displays a decreased succinate dehydrogenase activity, an integral component of the mitochondrial respiratory chain (complex II), and increased oxidative stress during hindlimb suspension in rats [16]. Our previous study also demonstrates that mitochondrial dislocation during unloading conditions has deleterious effects on muscle fibers leading to atrophy and ROS leakage from the mitochondria [6]. Therefore, muscle atrophy stimulated by unloading stress in tail suspension is associated with the disturbance of mitochondrial ability including mitochondrial oxidative phosphorylation.

Numerous reports have proven that AX exerts its effects on mitochondria in fatty-liver disease, caused due to a high-fat diet, nonalcoholic steatohepatitis [31, 32], gastric inflammation by oxidative stress [33], and cardiovascular diseases [34, 35]. These unique characteristics of AX on mitochondria may relate to itself membrane structure. AX consists of conjugated double bonds, hydroxyl, and keto groups that can embed in the cell membrane, from the inside to outside. This feature confers strong antioxidant activity, which enables AX to react with the free radicals [36, 37]. Our results indicated that AX was preferentially detected in the mitochondrial fraction and is consistent with previous reports of its accumulation in the mitochondria of normal human mesangial cells and blastocysts [12, 22]. These findings strengthened the possibility that AX reacted to ROS produced from mitochondrial respiratory chain complexes, leading to the prevention of oxidative stress-related diseases, including muscle atrophy.

AnA is an inhibitor of the mitochondrial respiratory chain complex III, a major site of mitochondrial ROS generation, and strongly activates the production and release of superoxide anions into the inner mitochondria membrane space [38]. We examined the effect of AX on AnA-induced mitochondrial O^{2-} production using succinate as a complex II substrate. AX significantly

Preprints (www.preprints.org) | NOT PEER-REVIEWED | Posted: 17 June 2020 doi:10.20944/preprints202006.0222.v1

suppressed mitochondrial complex III-driven ROS production in Sol8 myotubes (Figure. 5a), whereas its effect was not observed in C2C12 myotubes (data not shown), which is likely to be involved in muscle fiber type. Sole8 and C2C12 cells were derived from SO and adult dystrophic mouse muscles, respectively. Indo et al. showed that the SO muscle, which is enriched with slow-twitch fibers, exhibits a higher production of ROS than fast-twitch fibers [3]. Some studies have also reported that dietary antioxidants reduce ROS production and ameliorate atrophy in the SO muscle more than other fast-twitch fibers [39-41]. These results indicate that AX could target the mitochondria to eliminate O^{2-} production and inhibit muscle atrophy induced due to mitochondrial oxidative stress in slow-twitch fibers.

Loss of MMP and excess ROS production in mitochondria leads to cytochrome c release from the mitochondria into the cytosol, resulting in the induction of apoptosis [42-46]. It has been revealed that overproduction of mitochondrial ROS, mitochondrial dysfunction, and mitochondria-mediated apoptosis play vital roles in skeletal muscle atrophy [47, 48]. Caspase 3 is downstream of cytochrome c; the release of cytochrome c activates caspase 3, which induces apoptosis [49, 50]. It has been reported that a deficiency in caspase 3 prevents denervation-induced muscle atrophy [51]. In our present study, AX showed improvement of disturbed MMP as well as increased mitochondrial ROS by AnA treatment, thereby inactivation of caspase 3 through an inhibition of cytochrome c release into cytosol in Sol8 myotubes. In agreement with this finding, AX has been shown to protect against decreased MMP by virtue of improving mitochondrial function in cancer and neural cells [11, 52]. These results suggested that AX targeted and protected mitochondria by scavenging free oxygen radicals, regulating MMP, and inhibiting apoptosis in muscle cells.

5. Conclusions

In summary, the current study revealed that AX prevented muscle atrophy in slow-type muscles (SO). The direct effect of AX on mitochondria brought about the reduction of oxidative stress, regulation of MMP, and attenuation of apoptosis. These effects could collectively prevent the onset of muscle atrophy. Based on these results, AX could be considered as a potential treatment option for muscle atrophy and mitochondria-related diseases.

Author Contributions: Conceptualization, L.S., and K.H.; Data curation, L.S., N.M., M.Y., E.M.M., S.T., T.U., T.N., J.L., J.S., K. T., and K.H.; Formal analysis, L. S., and K.H.; Funding acquisition, K.H.; Investigation, L.S., M.Y., and K.H.; Methodology, L.S., M. Y., E.M.M., and K.H.; Project administration, K.H.; Resources, N.M.; Validation, L.S., and K.H; Writing—original draft, L.S. and K.H.; Writing—review and editing, L.S., E.M.M., and K.H. All authors have read and agreed to the published version of the manuscript.

Funding: This work was supported by Grant-in-Aid for Scientific Research of Japan (KAKENHI) (Grant Number: 19K11792).

Acknowledgments: We would like to thank Editage (www.editage.com) for English language editing.

Conflicts of Interest: The authors declare no conflict of interest.

Abbreviations:

AnA	antimycin A
ATP	adenosine triphosphate
AX	astaxanthin
CCCP	cytochrome cyanide m-chlorophenyl
CSA	cross-sectional area
DHE	dihydroethidium
DMEM	Dulbecco's modified eagle medium
DMSO	dimethyl sulfoxide
EDL	extensor digitorum longus

EDTA	ethylenediaminetetraacetic acid
FBS	fetal bovine serum
GA	gastrocnemius
HBSS	Hank's balanced salt solutions
HPLC	high performance liquid chromatography
HS	horse serum
MHC	myosin heavy chain
MMP	mitochondrial membrane potential
OXPHOS	oxidative phosphorylation
PVDF	polyvinylidene difluoride
ROS	reactive oxygen species
SDS-PAGE	odium dodecyl sulfate - polyacrylamide gel electrophoresis
SO	soleus
TA	tibialis anterior

References

1. Goto, K.; Okuyama, R.; Honda, M.; Uchida, H.; Akema, T.; Ohira, Y.; Yoshioka, T. Profiles of Connectin (Titin) in Atrophied Soleus Muscle Induced by Unloading of Rats. *J. Appl. Physiol. (1985)* **2003**, 94(3), 897-902.
2. Ohira, Y. Neuromuscular Adaptation to Microgravity Environment. *Jpn. J. Physiol.* **2000**, 50(3), 303-14.
3. Indo, H.P.; Davidson, M.; Yen, H.C.; Suenaga, S.; Tomita, K.; Nishii, T.; Higuchi, M.; Koga, Y.; Ozawa, T.; Majima, H.J. Evidence of ROS Generation by Mitochondria in Cells with Impaired Electron Transport Chain and Mitochondrial DNA Damage. *Mitochondrion* **2007**, 7(1-2), 106-18.
4. Chance, B.; Sies, H.; Boveris, A. Hydroperoxide Metabolism in Mammalian Organs. *Physiol. Rev.* **1979**, 59(3), 527-605.
5. Powers, S.K.; Smuder, A.J.; Criswell, D.S. Mechanistic Links Between Oxidative Stress and Disuse Muscle Atrophy. *Antioxid Redox Signal* **2011**, 15(9), 2519-28.
6. Nikawa, T.; Ishidoh, K.; Hirasaka, K.; Ishihara, I.; Ikemoto, M.; Kano, M.; Kominami, E.; Nonaka, I.; Ogawa, T.; Adams, G.R.; Baldwin, K.M.; Yasui, N.; Kishi, K.; Takeda, S. Skeletal Muscle Gene Expression in Space-Flown Rats. *FASEB. J.* **2004**, 18(3), 522-4.
7. Davinelli, S.; Nielsen, M.E.; Scapagnini, G. Astaxanthin in Skin Health, Repair, and Disease: A Comprehensive Review. *Nutrients* **2018**, 22, 10(4), 522.
8. Yuan, J.P.; Peng, J.; Yin, K.; Wang, J.H. Potential Health-Promoting Effects of Astaxanthin: A High-Value Carotenoid Mostly From Microalgae. *Mol. Nutr. Food. Res.* **2011**, 55(1), 150-65.
9. Ohno, M.; Darwish, W.S.; Ikenaka, Y.; Miki, W.; Ishizuka, M. Astaxanthin Can Alter CYP1A-dependent Activities via Two Different Mechanisms: Induction of Protein Expression and Inhibition of NADPH P450 Reductase Dependent Electron Transfer. Food Chem. *Toxicol.* **2011**, 49(6), 1285-91.
10. Wolf, A.M.; Asoh, S.; Hiranuma, H.; Ohsawa, I.; Iio, K.; Satou, A.; Ishikura, M.; Ohta, S. Astaxanthin Protects Mitochondrial Redox State and Functional Integrity Against Oxidative Stress. *J. Nutr. Biochem.* **2010**, 21(5), 381-9.
11. Zhang, Z.W.; Xu, X. C.; Liu, T.; Yuan, S. Mitochondrion-Permeable Antioxidants to Treat ROS-Burst-Mediated Acute Diseases. Oxid. Med. *Cell Longev.* **2016**, 1, 6859523.
12. Kuroki, T.; Ikeda, S.; Okada, T.; Maoka, T.; Kitamura, A.; Sugimoto, M.; Kume, S.; Astaxanthin Ameliorates Heat Stress-Induced Impairment of Blastocyst Development in Vitro: --Astaxanthin Colocalization With and Action on Mitochondria--. *J. Assist Reprod Genet.* **2013**, 30(5), 623-31.

13. Song, X.D.; Wang, B.S.; Lin, S.C.; Jing, L.L.; Mao, C.P.; Xu, P.; Lv, C.J.; Liu, W.; Zuo, J. Astaxanthin Inhibits Apoptosis in Alveolar Epithelial Cells Type II in Vivo and in Vitro Through the ROS-dependent Mitochondrial Signalling Pathway. *J. Cell. Mol. Med.* **2014**, 18(11), 2198-212.
14. Mukai, R.; Matsui, N.; Fujikura, Y.; Matsumoto, N.; Hou, D.X.; Kanzaki, N.; Shibata, H.; Horikawa, M.; Iwasa, K.; Hirasaka, K.; Nikawa, T.; Terao, J. Preventive Effect of Dietary Quercetin on Disuse Muscle Atrophy by Targeting Mitochondria in Denervated Mice. *J. Nutr. Biochem.* **2016**, 31, 67-76.
15. Hiramoto, S.; Yahata, N.; Saitoh, K.; Yoshimura, T.; Wang, Y.; Taniyama, S.; Nikawa, T.; Tachibana, K.; Hirasaka, K. Dietary Supplementation With Alkylresorcinols Prevents Muscle Atrophy Through a Shift of Energy Supply. *J. Nutr. Biochem.* **2018**, 61, 147-154.
16. Kanazashi, M.; Tanaka, M.; Nakanishi, Y.; Maeshige, N.; Fujino H. Effects of Astaxanthin Supplementation and Electrical Stimulation on Muscle Atrophy and Decreased Oxidative Capacity in Soleus Muscle During Hindlimb Unloading in Rats. *J. Physiol. Sci.* **2019**, 69(5), 757-767.
17. Shibaguchi, T.; Yamaguchi, Y.; Miyaji, N.; Yoshihara, T.; Naito, H.; Goto, K.; Ohmori, D.; Yoshioka, T.; Sugiura, T. Astaxanthin Intake Attenuates Muscle Atrophy Caused by Immobilization in Rats. *Physiol. Rep.* **2016**, 4(15), e12885.
18. Bloemberg, D.; Quadrilatero, J. Rapid Determination of Myosin Heavy Chain Expression in Rat, Mouse, and Human Skeletal Muscle Using Multicolor Immunofluorescence Analysis. *PLoS One* **2012,** 7(4), e35273.
19. Sprague, J.E.; Yang, X.M.; Sommers, J.; Gilman, T.L.; Mills, E.M. Roles of Norepinephrine, Free Fatty Acids, Thyroid Status, and Skeletal Muscle Uncoupling Protein 3 Expression in Sympathomimetic-Induced Thermogenesis. *J. Pharmacol. Exp. Ther.* **2007**, 320(1), 274-80.
20. Hirasaka, K.; Lago, C.U.; Kenaston, M.A.; Fathe, K.; Nowinski, S.M.; Nikawa, T.; Mills, E.M. Identification of a Redox-Modulatory Interaction Between Uncoupling Protein 3 and Thioredoxin 2 in the Mitochondrial Intermembrane Space. *Antioxid Redox Signal* **2011**, 15(10), 2645-61.
21. Kitaoka, Y.; Takeda, K.; Tamura, Y.; Fujimaki, S.; Takemasa, T.; Hatta, H. Nrf2 Deficiency Does Not Affect Denervation-Induced Alterations in Mitochondrial Fission and Fusion Proteins in Skeletal Muscle. *Physiol. Rep.* **2016**, 4(24), e13064.
22. Manabe, E.; Handa, O.; Naito, Y.; Mizushima, K.; Akagiri, S.; Adachi, S.; Takagi, T.; Kokura, S.; Maoka, T.; Yoshikawa, T. Astaxanthin Protects Mesangial Cells From Hyperglycemia-Induced Oxidative Signaling. *J. Cell. Biochem.* **2008**, 103(6), 1925-37.
23. Musacchia, X.J.; Steffen, J.M.; Deavers, D.R. Rat Hindlimb Muscle Responses to Suspension Hypokinesia/Hypodynamia. *Aviat. Space Environ. Med.* **1983**, 54(11), 1015-20.
24. Desplanches, D.; Mayet, M.H.; Sempore, B.; Flandrois, R. Structural and Functional Responses to Prolonged Hindlimb Suspension in Rat Muscle. *J. Appl. Physiol. (1985)* **1987**, 63(2), 558-63.
25. Marzetti, E.; Hwang, J.C.Y.; Lees, H.A.; Wohlgemuth, S.E.; Dupont-Versteegden, E.E.; Carter, C.S.; Bernabei, R.; Leeuwenburgh, C. Mitochondrial Death Effectors: Relevance to Sarcopenia and Disuse Muscle Atrophy. *Biochim. Biophys. Acta.* **2010**, 1800(3), 235-44.
26. Adhihetty, P.J.; Ljubicic, V.; Menzies, K.J.; Hood, D.A. Differential Susceptibility of Subsarcolemmal and Intermyofibrillar Mitochondria to Apoptotic Stimuli. *Am. J. Physiol. Cell. Physiol.* **2005**, 289(4), C994-C1001.
27. Romanello, V.; Guadagnin, E.; Gomes, L.; Roder, I.; Sandri, C.; Petersen, Y.; Milan, G.; Masiero, E.; Piccolo, P.D.; Foretz, M.; Scorrano, L.; Rudolf, R.; Sandri, M. Mitochondrial Fission and Remodelling Contributes to Muscle Atrophy. *EMBO. J.* **2010**, 29(10), 1774-85.
28. Romanello, V.; Sandri, M. Mitochondrial Biogenesis and Fragmentation as Regulators of Protein Degradation in Striated Muscles. *J. Mol. Cell. Cardiol.* **2013**, 55, 64-72.
29. Brand, M.D. The Sites and Topology of Mitochondrial Superoxide Production. *Exp. Gerontol.* **2010**, 45(7-8), 466-72.
30. Choi, M.H.; Ow, J.R.; Yang, N.D. Taneja, R. Oxidative Stress-Mediated Skeletal Muscle Degeneration: Molecules, Mechanisms, and Therapies. *Oxid. Med. Cell. Longev.* **2016**, 6842568.
31. Bhuvaneswari, S.; Anuradha, C.V. Astaxanthin Prevents Loss of Insulin Signaling and Improves Glucose Metabolism in Liver of Insulin Resistant Mice. *Can. J. Physiol. Pharmacol.* **2012**, 90(11), 1544-52.
32. Ni, Y.; Nagashimada, M.; Zhuge, F.; Zhan, L.L.; Nagata N.; Tsutsui, A.; Nakanuma, Y.; Kaneko, S. Ota, T. Astaxanthin Prevents and Reverses Diet-Induced Insulin Resistance and Steatohepatitis in Mice: A Comparison With Vitamin E. *Sci. Rep.* **2015**, 5, 17192.
33. Kim, S.H.; Lim, J.W.; Kim, H. Astaxanthin Inhibits Mitochondrial Dysfunction and Interleukin-8 Expression in Helicobacter pylori-Infected Gastric Epithelial Cells. *Nutrients* **2018**, 10(9), 1320.

34. Fan, C.D.; Sun, J.Y.; Fu, X.T.; Hou, Y.J.; Li, Y. Yang, M.F.; Fu, X.Y.; Sun, B.Y. Astaxanthin Attenuates Homocysteine-Induced Cardiotoxicity in Vitro and in Vivo by Inhibiting Mitochondrial Dysfunction and Oxidative Damage. *Front. Physiol.* **2017**, 8, 1041.
35. Krestinina, O.; Baburina, Y.; Krestinin, R.; Odinokova, I.; Fadeeva, I.; Sotnikova L. Astaxanthin Prevents Mitochondrial Impairment Induced by Isoproterenol in Isolated Rat Heart Mitochondria. *Antioxidants (Basel)* **2020**, 9(3), 262.
36. Higuera-Ciapara, I. Félix-Valenzuela, L.; Goycoolea, F.M. Astaxanthin: A Review of Its Chemistry and Applications. *Crit. Rev. Food Sci. Nutr*. **2006**, 46(2), 185-96.
37. Ambati, R.R.; Phang, S.M.; Ravi, S.; Aswathanarayana, R.G. Astaxanthin: Sources, Extraction, Stability, Biological Activities and Its Commercial Applications--A Review. *Mar. Drugs* **2014**, 12(1), 128-52.
38. Turrens, J.F.; Alexandre, A.; Lehninger, A.L. Ubisemiquinone Is the Electron Donor for Superoxide Formation by Complex III of Heart Mitochondria. *Arch. Biochem. Biophys.* **1985**, 237(2), 408-14.
39. Kitakaze, T.; Harada, N.; Imagita, H.; Yamaji, R. β-Carotene Increases Muscle Mass and Hypertrophy in the Soleus Muscle in Mice. *J. Nutr. Sci. Vitaminol (Tokyo)* **2015**, 61(6), 481-7.
40. Ogawa, M.; Kariya, Y.; Kitakaze, T.; Yamaji, R.; Harada, N.; Sakamoto, T.; Hosotani, K.; Nakano, Y.; Inui, H. The Preventive Effect of β-Carotene on Denervation-Induced Soleus Muscle Atrophy in Mice. *Br. J. Nutr.* **2013**, 109(8), 1349-58.
41. Yoshihara, T.; Yamamoto, Y.; Shibaguchi, T.; Miyaji, N.; Kakigi, R.; Naito, H.; Goto, K.; Ohmori, D.; Yoshioka, T.; Sugiura, T. Dietary Astaxanthin Supplementation Attenuates Disuse-Induced Muscle Atrophy and Myonuclear Apoptosis in the Rat Soleus Muscle. *J. Physiol. Sci.* **2017**, 67(1), 181-190.
42. Li, J.; Yu, W.; Li, X.T.; Qi, S.H.; Li, B. The Effects of Propofol on Mitochondrial Dysfunction Following Focal Cerebral Ischemia-Reperfusion in Rats. *Neuropharmacology* **2014**, 77, 358-68.
43. He, G.D.; Feng, C.; Vinothkumar, R.; Chen, W.Q.; Dai, X.X.; Chen, X.; Ye, Q.Q.; Qiu, C.Y.; Zhou, H.P.; Wang, Y.; Liang, G.; Xie, Y.B.; Wu, W. Curcumin Analog EF24 Induces Apoptosis via ROS-dependent Mitochondrial Dysfunction in Human Colorectal Cancer Cells. *Cancer Chemother Pharmacol* **2016**, 78(6), 1151-1161.
44. Shanmugapriya, K.; Kim, H.; Kang, H.W. In Vitro Antitumor Potential of Astaxanthin Nanoemulsion Against Cancer Cells via Mitochondrial Mediated Apoptosis. *Int. J. Pharm.* **2019**, 560, 334-346.
45. Pajaniradje, S.; Mohankumar, K.; Pamidimukkala, R.; Subramanian, S.; Rajagopalan, R. Antiproliferative and Apoptotic Effects of Sesbania Grandiflora Leaves in Human Cancer Cells. *Biomed Res. Int.* **2014**, 474953.
46. Meghani, N.; Patel, P.; Kansara, K.; Ranjan, S.; Dasgupta,N.; Ramalingam, C.; Kumar, A. Formulation of Vitamin D Encapsulated Cinnamon Oil Nanoemulsion: Its Potential Anti-Cancerous Activity in Human Alveolar Carcinoma Cells. *Colloids Surf. B Biointerfaces* **2018**, 166, 349-357.
47. Du, J.; Wang, X.N. Miereles, C.; Bailey, J.L.; Debigare, R.; Zheng, B.; Price, S.R.; Mitch, W.E. Activation of caspase-3 Is an Initial Step Triggering Accelerated Muscle Proteolysis in Catabolic Conditions. *J. Clin. Invest.* **2004**, 113(1), 115-23.
48. Powers, S.K.; Kavazis, A.N.; McClung, J.M. Oxidative Stress and Disuse Muscle Atrophy. *J. Appl. Physiol. (1985)* **2007**, 102(6), 2389-97.
49. Wu, Q.; Tang, Z.H.; Peng, J.; Liao, L.; Pan, L.H.; Wu, C.Y.; Jiang, Z.S.; Wang, G.X.; Liu, L. S. The Dual Behavior of PCSK9 in the Regulation of Apoptosis Is Crucial in Alzheimer's Disease Progression (Review). *Biomed Rep*. **2014**, 2(2), 167-171.
50. Yang, Q.S.; Guo, S.F.; Wang, S.; Qian, Y.W.; Tai, H.P.; Chen, Z.X. Advanced Glycation End Products-Induced Chondrocyte Apoptosis Through Mitochondrial Dysfunction in Cultured Rabbit Chondrocyte. *Fundam. Clin. Pharmacol.* **2015**, 29(1), 54-61.
51. Plant, P.J.; Bain, J.R.; Correa, J.E.; Woo, M.; Batt, J. Absence of caspase-3 Protects Against Denervation-Induced Skeletal Muscle Atrophy. *J. Appl. Physiol. (1985)* **2009**, 107(1), 224-34.
52. Liu, X.B.; Shibata, T.; Hisaka, S.; Osawa, T. Astaxanthin Inhibits Reactive Oxygen Species-Mediated Cellular Toxicity in Dopaminergic SH-SY5Y Cells via Mitochondria-Targeted Protective Mechanism. *Brain Res.* **2009**, 1254, 18-27.